Polaron effects on the dc- and ac-tunneling characteristics of molecular Josephson junctions

B. H. Wu,[1,*] J. C. Cao,[2] and C. Timm[3,†]

[1]*Department of Applied Physics, Donghua University, 2999 North Renmin Road, Shanghai 201620, China*

[2]*Key Laboratory of Terahertz Solid-State Technology, Shanghai Institute of Microsystem and Information Technology, Chinese Academy of Sciences, 865 Changning Road, Shanghai 200050, China*

[3]*Institute of Theoretical Physics, Technische Universität Dresden, 01062 Dresden, Germany*

(Received 16 November 2011; published 5 July 2012)

We study the interplay of polaronic effect and superconductivity in transport through molecular Josephson junctions. The tunneling rates of electrons are dominated by vibronic replicas of the superconducting gap, which show up as prominent features in the differential conductance for the dc and ac current. For relatively large molecule-lead coupling, a features that appears when the Josephson frequency matches the vibron frequency can be identified with an over-the-gap structure observed by Marchenkov *et al.* [Nat. Nanotech. **2**, 481 (2007)]. However, we are more concerned with the weak-coupling limit, where resonant tunneling through the molecular level dominates. We find that certain features involving both Andreev reflection and vibron emission show an unusual shift of the bias voltage V at their maximum with the gate voltage V_g as $V \sim (2/3)\, V_g$. Moreover, due to the polaronic effect, the ac Josephson current shows a phase shift of π when the bias eV is increased by one vibronic energy quantum $\hbar\omega_v$. This distinctive even-odd effect is explained in terms of the different sign of the coupling to vibrons of electrons and of Andreev-reflected holes.

DOI: 10.1103/PhysRevB.86.035406 PACS number(s): 74.78.Na, 74.25.fc, 74.45.+c, 74.50.+r

I. INTRODUCTION

Electron transport through quantum dots embedded in Josephson junctions is attracting increasing interest.[1,2] Rich phenomena[3–9] arise due to the competition of superconductivity and strong interactions. A crucial feature of molecular Josephson junctions (MJJs) is the interplay of the ac Josephson effect and molecular vibrations. Signatures in the transport can be expected when the Josephson frequency matches a vibration frequency. Since the Josephson frequency can be precisely controlled by the bias voltage, such signatures could form the basis of a precise molecular spectroscopy. This idea has recently been explored by Marchenkov *et al.*,[6] who have measured the differential conductance of a Nb dimer in a superconducting break junction. An over-the-gap structure consisting of a series of peaks was ascribed to the excitation of vibrational modes by the ac Josephson current,[6] but no microscopic description was provided. Theoretical treatments of MJJs have mainly focused on the dc current either for weak molecule-lead coupling at vanishing bias[3] or for weak electron-vibron coupling[5,8] so that the microscopic understanding of spectroscopic signatures in transport through MJJs is still far from complete. However, such an understanding is the prerequisite for developing the dc and ac Josephson currents in MJJs into spectroscopic tools.

The purpose of this paper is to investigate the transport properties of a biased MJJ within a microscopic model. We focus on MJJs with strong electron-vibron coupling. In this limit, electrons dress with a vibron cloud, forming polarons. A minimal model of a single-orbital molecule between two s-wave superconducting leads is considered. Electrons in the molecular orbital are coupled to a vibrational mode of frequency ω_v. We will see that signatures in transport do not only occur when the Josephson frequency ω_J equals the vibration frequency ω_v but also when $\hbar\omega_J$, $\hbar\omega_v$, and the superconducting gap in the leads satisfy certain other simple rational relations.

The remainder of this paper is organized as follows: In Sec. II we present our model and discuss the theoretical approach. In Sec. III we then present and discuss our results for the dc and ac Josephson effects, followed by a summary in Sec. IV.

II. MODEL AND METHOD

Our model Hamiltonian reads

$$H = \sum_{\alpha=L,R} H_\alpha + H_{\rm mol} + H_T, \tag{1}$$

where the first term describes the left (L) and right (R) BCS superconducting leads,

$$H_\alpha = \sum_{\mathbf{k}\sigma} \epsilon_{\alpha\mathbf{k}\sigma}\, c^\dagger_{\alpha\mathbf{k}\sigma} c_{\alpha\mathbf{k}\sigma} + \sum_{\mathbf{k}\sigma} (\Delta^*_\alpha\, c_{\alpha\mathbf{k}\uparrow} c_{\alpha,-\mathbf{k},\downarrow} + \text{H.c.}), \tag{2}$$

with superconducting order parameter Δ_α. $c_{\alpha\mathbf{k}\sigma}$ ($c^\dagger_{\alpha\mathbf{k}\sigma}$) annihilates (creates) an electron of wave vector $\mathbf{k}$ and spin σ in lead α.

The molecule with vibration degree of freedom is represented by

$$H_{\rm mol} = \sum_\sigma \varepsilon_m d^\dagger_\sigma d_\sigma + \hbar\omega_v a^\dagger a + \lambda(a^\dagger + a) \sum_\sigma d^\dagger_\sigma d_\sigma, \tag{3}$$

where ε_m is the molecular energy level, d_σ ($d^\dagger_\sigma$) is the annihilation (creation) operator of a spin-σ electron in the molecular orbital, a ($a^\dagger$) is the vibron annihilation (creation) operator, and λ is the electron-vibron coupling strength. We neglect the Coulomb interaction in the molecule, which is justified if the charging energy is small compared to the coupling to the leads.[10] The role of the Coulomb interaction in MJJs has recently been reviewed in Ref. 1.

The tunneling between the molecule and the leads is described by

$$H_T = \frac{1}{\sqrt{N}} \sum_{\alpha \mathbf{k}\sigma} t_{\alpha d} \exp\left[\frac{i}{2}\left(\phi_\alpha + \frac{2eV_\alpha}{\hbar} t\right)\right] c^\dagger_{\alpha \mathbf{k}\sigma} d_\sigma + \text{H.c.}, \tag{4}$$

where ϕ_α is the initial phase of the superconducting order parameter at time $t = 0$, V_α is the voltage in lead α, and $t_{\alpha d}$ is the tunneling matrix element. In the following we choose $\phi_\alpha = 0$, $V_L = 0$, and $V_R = -V$, where V is the voltage drop across the junction. For symmetric capacitances between the molecule and the leads, as assumed here, the molecular energy level is then given by $\varepsilon_m = \varepsilon_0 - eV/2$.

To go beyond perturbative approaches,[3,5,8] we employ the unitary Lang-Firsov transformation[11–13] to diagonalize H_{mol}. The transformed Hamiltonian reads

$$\tilde{H} = H_\alpha + \sum_\sigma \left(\tilde{\varepsilon}_0 - \frac{eV}{2}\right) d^\dagger_\sigma d_\sigma + \hbar\omega_v\, a^\dagger a + \tilde{H}_T, \tag{5}$$

where the molecular energy level is shifted to $\tilde{\varepsilon}_0 = \varepsilon_0 - \lambda^2/\hbar\omega_v$ by the polaron binding energy. To simplify notation we now take ε_0 to denote the shifted level. In principle, the electron-electron interaction is also renormalized by the transformation but we neglect this shift together with the bare Coulomb interaction. We do not expect the on-site interaction to qualitatively change our results, which are concerned with transport outside of the Coulomb-blockade regime. $\tilde{H}_T$ has the same form as H_T, except that the tunneling matrix elements are dressed by the polaronic effect as $\tilde{t}_{\alpha d} = t_{\alpha d} X$, where

$$X = \exp\left[-\frac{\lambda}{\hbar\omega_v}(a^\dagger - a)\right] \tag{6}$$

is the polaron-shift operator.

The transport properties are obtained by the nonequilibrium-Green-function method.[12,14] In the Nambu representation we introduce the contour-ordered Green function $G(t,t') = -i\langle T_c\, \psi(t)\psi^\dagger(t')\rangle$ with the contour-ordering directive T_c and $\psi = (d_\uparrow, d^\dagger_\downarrow)^T$. The particle current through the lead α is[14–16]

$$I_\alpha(t) = \frac{2e}{\hbar}\,\text{Re}\int dt_1\,\text{Tr}\left\{\sigma_z\left[G^<(t,t_1)\Sigma^a_\alpha(t_1,t) + G^r(t,t_1)\Sigma^<_\alpha(t_1,t)\right]\right\}, \tag{7}$$

where the trace is over Nambu space, σ_z is a Pauli matrix, and Σ^a_α and $\Sigma^<_\alpha$ are, respectively, the advanced and lesser self-energies due to the coupling to lead α. The advanced self-energy is related to the retarded one through $\Sigma^a(t,t') = [\Sigma^r(t',t)]^\dagger$.

The current measured in, say, the left lead consists of the particle current $I_L(t)$ plus the displacement current due to the formation of image charges. This contribution vanishes in the stationary state but must be taken into account in the time-dependent case to ensure gauge invariance and current conservation. This requires proper partitioning of the displacement current.[17] Since we assume symmetric coupling, the displacement currents are symmetric, in which case the measured current equals the symmetrized current $I = (I_L - I_R)/2$.[17,18] Due to the ac Josephson effect, the current can be expanded as $I(t) = \sum_n I_n e^{in\omega_J t}$, where the Josephson frequency is $\omega_J = 2eV/\hbar$ and $I_n = (I_{L,n} - I_{R,n})/2$. The Fourier components $I_{\alpha,n}$ are

$$I_{\alpha,n} = \frac{2e}{h}\int d\epsilon\,\text{Re}\,\text{Tr}\sum_m \left\{\sigma_z\left[G^<_{-n,m}(\epsilon)\,\Sigma^a_{\alpha;m,0}(\epsilon) + G^r_{-n,m}(\epsilon)\,\Sigma^<_{\alpha;m,0}(\epsilon)\right]\right\}, \tag{8}$$

where $G_{m,n}(\epsilon) \equiv G_{n-m}(\epsilon + m\omega_J)$ and

$$G_n(\epsilon) \equiv \int_{-\infty}^{\infty} dt\,\frac{1}{T}\int_0^T dt'\, e^{i\epsilon(t-t')}\, e^{-in\omega_J t'}\, G(t,t') \tag{9}$$

and analogously for the self-energies. The current can be decomposed into dissipative (I^D_n) and nondissipative (I^S_n) contributions,[15,16]

$$I(t) = I_0 + \sum_{n>0}\left(I^D_n \cos n\omega_J t + I^S_n \sin n\omega_J t\right), \tag{10}$$

where $I^D_n = \text{Re}\,(I_{-n} + I_n)$ and $I^S_n = \text{Im}\,(I_{-n} - I_n)$.

Before turning to transport properties, we show that the molecule-lead coupling is drastically modified by the polaronic effect. We employ the standard decoupling approximation, which assumes that averages of products of two polaron-shift operators can be taken out of electronic Green functions and evaluated in equilibrium.[12,19–21] This approximation is valid if $\hbar\omega_v$ or λ is large compared to the molecule-lead coupling. It is known that beyond its range of quantitative reliability, the approximation predicts resonant features that are too broad and too low, but that are centered at the same energy as obtained from a more advanced treatment.[21] In contrast to previous studies for normal leads, we encounter not only the correlation function $\langle X(t-t')X^\dagger\rangle$ but also $\langle X(t-t')X\rangle$. These functions are given by[12,13,20,21]

$$\langle X(t)X^\dagger\rangle = \langle X^\dagger(t)X\rangle = \sum_l L_l\, e^{-in\omega_v t}, \tag{11}$$

$$\langle X(t)X\rangle = \langle X^\dagger(t)X^\dagger\rangle = \sum_l (-1)^l\, L_l\, e^{-in\omega_v t}, \tag{12}$$

where

$$L_l \equiv e^{-(\lambda/\hbar\omega_v)^2(2N_v+1)} \exp\left(\frac{l\hbar\omega_v}{2k_B T}\right) I_l(\eta), \tag{13}$$

with the modified Bessel function I_l of the argument $\eta = 2(\lambda/\hbar\omega_v)^2\sqrt{N_v(N_v+1)}$. N_v is the average vibron number at temperature T determined by the Bose-Einstein distribution function. The correlation functions can be evaluated analytically. While the normal one has the well-known form[12,13,20,21]

$$\langle X(t)X^\dagger\rangle = \exp\{-g^2\left[(1 - e^{-i\omega_v t})(N_v+1) + N_v(1 - e^{i\omega_v t})\right]\}, \tag{14}$$

the anomalous one is

$$\langle X(t)X\rangle = \exp\{-g^2\left[(1 + e^{-i\omega_v t})(N_v+1) + N_v(1 + e^{i\omega_v t})\right]\}. \tag{15}$$

The two correlation functions differ by a phase shift of half a vibration period. This phase shift will turn out to be crucial for the polaron effect on the Josephson current. Its origin can be traced back to the factor of $(-1)^l$ under the sum in Eq. (12). This factor stems from Andreev reflection: An electron tunneling out of the molecule transmutes into a hole before it tunnels back in, which couples to the vibron *with the opposite sign*, as seen by inspecting the last term in Eq. (3).

Under the decoupling approximation, we obtain the retarded and lesser self-energies due to the coupling to superconducting lead α as

$$\begin{aligned}\left[\Sigma^r_{\alpha;mn}\right]_{ij}(\epsilon) &= \sum_{l=-\infty}^{\infty}(-1)^{l(i-j)}L_l\Big\{\left[\tilde{\Sigma}^r_{\alpha;mn}\right]_{ij}(\epsilon_l^-) \\ &+\frac{1}{2}\left([\tilde{\Sigma}^<_{\alpha;mn}]_{ij}(\epsilon_l^-)-[\tilde{\Sigma}^<_{\alpha;mn}]_{ij}(\epsilon_l^+)\right) \\ &+\frac{1}{2i}(H[[\tilde{\Sigma}^<_{\alpha;mn}]_{ij}](\epsilon_l^-)-H[[\tilde{\Sigma}^<_{\alpha;mn}]_{ij}](\epsilon_l^+))\Big\} \quad (16)\end{aligned}$$

and

$$[\Sigma^<_{\alpha;mn}]_{ij}=\sum_{l=-\infty}^{\infty}(-1)^{l(i-j)}L_l\,[\tilde{\Sigma}^<_{\alpha;mn}]_{ij}(\epsilon+l\omega_v), \quad (17)$$

respectively, where $\epsilon_l^{\pm}\equiv\epsilon\pm l\hbar\omega_v$, and $i,j=1,2$ are Nambu indices. Here, $\tilde{\Sigma}_\alpha$ is the self-energy in the absence of electron-vibron coupling. Taking the wide-band limit and making use of our choice of vanishing initial phases ϕ_α at time $t=0$, $\tilde{\Sigma}_\alpha$ is given by[15,16]

$$\tilde{\Sigma}^r_{L;mn}(\epsilon)=-\frac{i}{2}\,\Gamma_L\,\beta_L(\tilde{\epsilon}_m)\begin{pmatrix}1 & -\frac{\Delta_L}{\tilde{\epsilon}_m}\\ -\frac{\Delta_L}{\tilde{\epsilon}_m} & 1\end{pmatrix}, \quad (18)$$

$$\tilde{\Sigma}^r_{R;mn}(\epsilon)=-\frac{i}{2}\,\Gamma_R\begin{pmatrix}\delta_{mn}\,\beta_R(\tilde{\epsilon}_{m+1/2}) & \delta_{m,n-1}\,\beta_R(\tilde{\epsilon}_{m+1/2})\,\frac{-\Delta_R}{\tilde{\epsilon}_{m+1/2}}\\ \delta_{m,n+1}\,\beta_R(\tilde{\epsilon}_{m-1/2})\,\frac{-\Delta_R}{\tilde{\epsilon}_{m-1/2}} & \delta_{mn}\,\beta_R(\tilde{\epsilon}_{m-1/2})\end{pmatrix}, \quad (19)$$

$$\tilde{\Sigma}^<_{L;mn}(\epsilon)=i\,\Gamma_L\,\delta_{mn}\,f(\tilde{\epsilon}_m)\,\tilde{\rho}_L(\tilde{\epsilon}_m)\begin{pmatrix}1 & -\frac{\Delta_L}{\tilde{\epsilon}_m}\\ -\frac{\Delta_L}{\tilde{\epsilon}_m} & 1\end{pmatrix}, \quad (20)$$

$$\tilde{\Sigma}^<_{R;mn}(\epsilon)=i\,\Gamma_R\begin{pmatrix}\delta_{mn}\,f(\tilde{\epsilon}_{m+1/2})\,\tilde{\rho}_R(\tilde{\epsilon}_{m+1/2}) & \delta_{m,n-1}\,f(\tilde{\epsilon}_{m+1/2})\,\tilde{\rho}_R(\tilde{\epsilon}_{m+1/2})\,\frac{-\Delta_R}{\tilde{\epsilon}_{m+1/2}}\\ \delta_{m,n+1}\,f(\tilde{\epsilon}_{m-1/2})\,\tilde{\rho}_R(\tilde{\epsilon}_{m-1/2})\,\frac{-\Delta_R}{\tilde{\epsilon}_{m-1/2}} & \delta_{mn}\,f(\tilde{\epsilon}_{m-1/2})\,\tilde{\rho}_R(\tilde{\epsilon}_{m-1/2})\end{pmatrix}, \quad (21)$$

where $\tilde{\epsilon}_m\equiv\epsilon+m\hbar\omega_J$ and $f(\epsilon)\equiv(e^{\epsilon/k_BT}+1)^{-1}$ is the Fermi-Dirac distribution function, where the chemical potential in the left lead is independent of the bias voltage due to our assumption of $V_L=0$ and has been absorbed into ϵ. The shifts in the arguments $\tilde{\epsilon}_{m\pm1/2}$ of the Fermi functions in Eq. (21) account for the potential difference between the leads. $\Gamma_\alpha\equiv2\pi|t_{\alpha d}|^2\rho_\alpha^N$ describes the coupling of the molecule to lead α, where ρ_α^N is the density of states in lead α in the normal state. In the wide-band limit, Γ_α is independent of energy. Also, for symmetric coupling we have $\Gamma_L=\Gamma_R\equiv\Gamma$. The expressions for β_α and $\tilde{\rho}_\alpha$ read

$$\beta_\alpha(\epsilon)=\begin{cases}\frac{\epsilon}{i\sqrt{\Delta_\alpha^2-\epsilon^2}} & \text{for}\quad \Delta_\alpha>|\epsilon|,\\ \frac{|\epsilon|}{\sqrt{\epsilon^2-\Delta_\alpha^2}} & \text{for}\quad \Delta_\alpha<|\epsilon|,\end{cases} \quad (22)$$

$$\tilde{\rho}_\alpha(\epsilon)=\theta(|\epsilon|-\Delta_\alpha)\,\frac{|\epsilon|}{\sqrt{\epsilon^2-\Delta_\alpha^2}}, \quad (23)$$

respectively. Furthermore,

$$H[F](\omega)\equiv\frac{1}{\pi}\,P\int d\epsilon\,\frac{F(\epsilon)}{\omega-\epsilon} \quad (24)$$

is the Hilbert transform of the function F, where P denotes the principal value. The above results are valid for fast vibron relaxation so that the averages of bosonic operators can be taken in equilibrium. Figure 1 shows $-\mathrm{Im}\,(\Sigma^r_L)_{11}$ for various electron-vibron coupling strengths λ. Without electron-vibron coupling, $-\mathrm{Im}\,(\Sigma^r_L)_{11}$ exhibits the superconducting gap of the left lead. In the presence of electron-vibron coupling, $-\mathrm{Im}\,(\Sigma^r_L)_{11}$ develops vibronic replicas of the gap edges, separated by integer multiples of $\hbar\omega_v$, which open inelastic transport channels beyond the usual Andreev reflection.[15,16] They enable electrons with energies above the superconducting gap to undergo Andreev reflection under emission or absorption of vibrons.

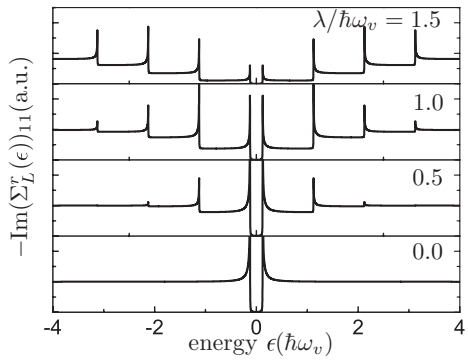

FIG. 1. Imaginary part of the first diagonal element of the retarded self-energy $-\mathrm{Im}\,(\Sigma^r_L)_{11}$, which represents scattering of electrons between the molecule and lead L, for various electron-vibron coupling strengths λ. We have taken $\hbar\omega_v=8\,\Delta$ and $\Gamma=0.2\,\hbar\omega_v$. With increasing λ, multiple vibronic replicas of the superconducting gap edges appear.

III. RESULTS AND DISCUSSION

A. Differential conductance of the dc Josephson current

We now discuss the modification of the Josephson current due to the polaronic effect. In this study we assume the two leads to be identical superconductors and take the amplitude of the order parameters to be $\Delta \equiv |\Delta_L| = |\Delta_R|$. In Fig. 2 we first present density plots of the dc differential conductance dI_0/dV as a function of the bias voltage V and the on-site energy ε_0, which in a break-junction setup could be controlled by a gate voltage. Different polaronic features are observed depending on the molecule-lead coupling Γ. For large Γ, dc transport is dominated by coherent tunneling across the molecule without requiring the energy of the electron to be aligned with the molecular level. For Fig. 2(a) we have chosen $\Gamma = \lambda = \hbar\omega_v$. As noted above, in this regime the decoupling approximation is expected to underestimate the polaronic effect on transport but to show resonances at the correct voltages.[21] The numerical results thus provide a reasonable qualitative description to the

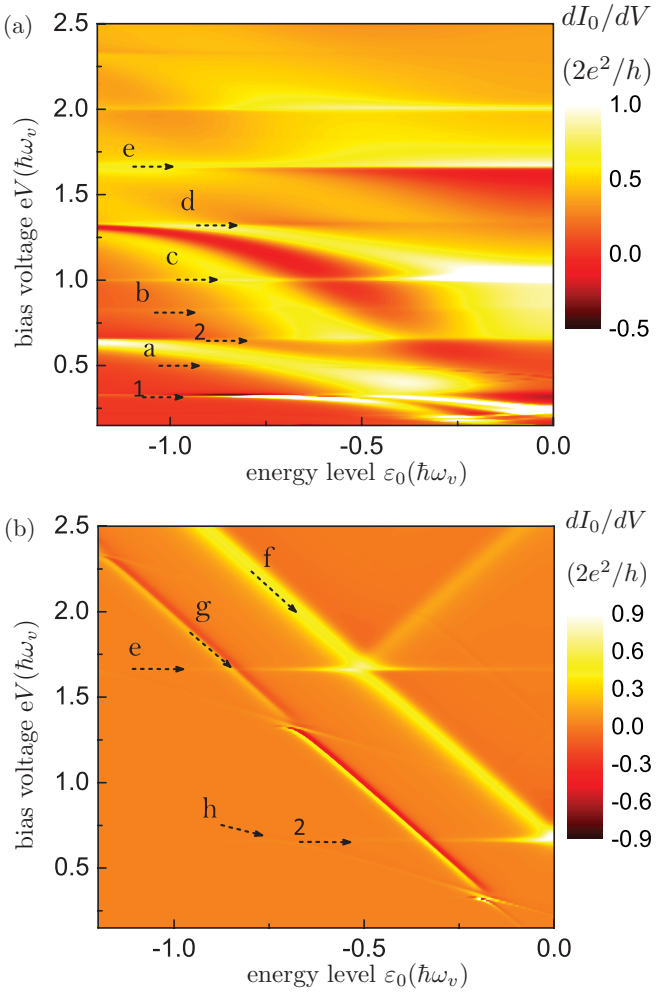

FIG. 2. (Color online) Density plot of the dc differential conductance dI_0/dV vs on-site energy ε_0 and bias voltage V for $\Delta = \hbar\omega_v/3$, $\lambda = \hbar\omega_v$, and (a) $\Gamma = \hbar\omega_v$ and (b) $\Gamma = 0.05\hbar\omega_v$. Features labeled "1" and "2" do not involve vibron emission or absorption, whereas those labeled "a"–"h" are due to this polaronic effect. All features are discussed in the text.

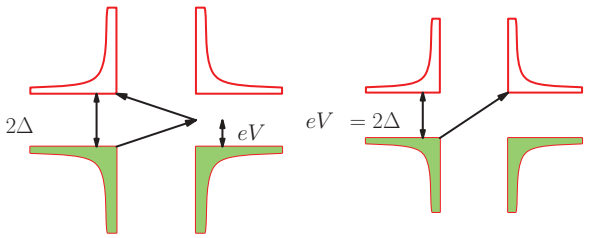

FIG. 3. (Color online) Schematic representations of the two most important processes in the MJJ that involve neither vibrons nor the molecular level. Left panel: single Andreev reflection at the right molecule-lead contact. Right panel: direct tunneling from the lower gap edge in the left lead to the upper gap edge in the right lead. The filled (empty) shapes represent the energy states of the superconducting leads below (above) the Fermi energy. Energy scales of the superconducting gap Δ and the bias voltage eV are indicated. The arrows denote possible transitions of the electron or hole.

vibron-assisted tunneling features. In Fig. 2(a) we find several features at fixed bias voltage, insensitive to ε_0. The feature labeled by "1" at $eV = \hbar\omega_v/3 = \Delta$ is due to single Andreev reflection without vibron emission or absorption. This process is illustrated by the left panel in Fig. 3. The feature labeled by "2" at $eV = 2\hbar\omega_v/3 = 2\Delta$ is due to direct tunneling from the lower gap edge at one side to the upper gap edge at the other, illustrated by the right panel in Fig. 3.

The features labeled by the letters "a"–"e" in Fig. 2(a) involve vibrons. All these features and their replicas shifted by integer multiples of $\hbar\omega_v$ can be explained by the onset of vibron-assisted Andreev reflections or coherent-tunneling processes sketched in Fig. 4, where the density of states (DOS) has been modified compared to the conventional picture of Andreev reflection[16,22,23] to account for the polaronic effect. For instance, the weak feature "a" located at $\omega_v = \omega_J$ arises from the resonance of the vibron and Josephson frequencies and has been invoked by Marchenkov *et al.*[6] to interpret the observed over-the-gap structure. The process is sketched in Fig. 4(a), where an electron from a singular edge of the left lead undergoes one Andreev reflection at the right lead and arrives at a singular edge of the left lead. In this process, one vibron is emitted.

On the other hand, for small Γ, where the decoupling approximation gives quantitatively reliable results, the tunneling processes are sensitive to the position of the molecular energy level. Pronounced features arise when singular edges of the DOS are aligned with the level ε_0. In Fig. 2(b) we show dI_0/dV vs V and ε_0 for weak coupling, $\Gamma = 0.05\hbar\omega_v$. As the nonresonant tunneling is strongly suppressed, the features seen in Fig. 2(a) become much weaker or are even invisible in Fig. 2(b). Instead we see vibron-induced features with peak bias voltages depending not only on ω_v and Δ but also on ε_0. Two features, labeled by "f" and "g," satisfy $\partial eV/\partial\varepsilon_0 = -2$. They are due to the alignment of the gap edges with the molecular level where resonant sequential tunneling through the molecule plays a dominant role. The corresponding processes are depicted in Figs. 4(f) and 4(g). Note that the level positions are renormalized due to the electron-vibron coupling. One can see that feature g displays a sharp rise in dI_0/dV followed by a narrow region of negative differential conductance. This is due to the onset

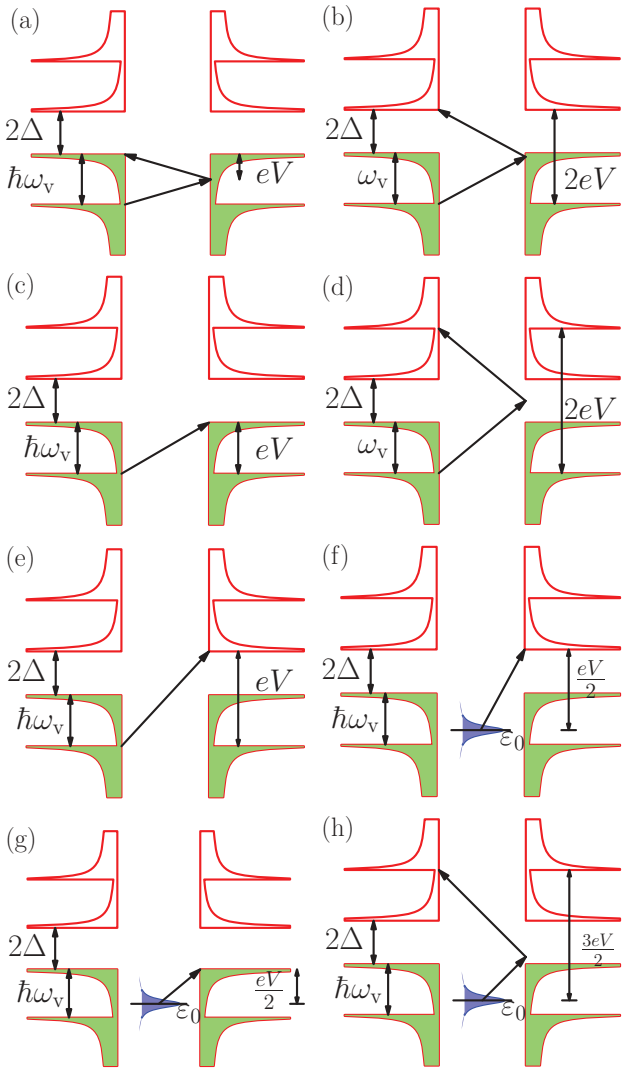

FIG. 4. (Color online) Schematic representation of various vibron-assisted tunneling and Andreev-reflection processes in the MJJ. The labels are the same as in Fig. 2. The DOS of both leads is modified due to the polaronic effect. The filled (empty) shapes represent the energy states of the superconducting leads below (above) the Fermi energy. The molecular level ϵ_0 (blue/gray) is broadened due to the coupling to the leads. Energy scales of the superconducting gap Δ, the vibron energy $\hbar\omega_v$, and the bias voltage eV are indicated. The arrows denote possible transitions of the electron or hole.

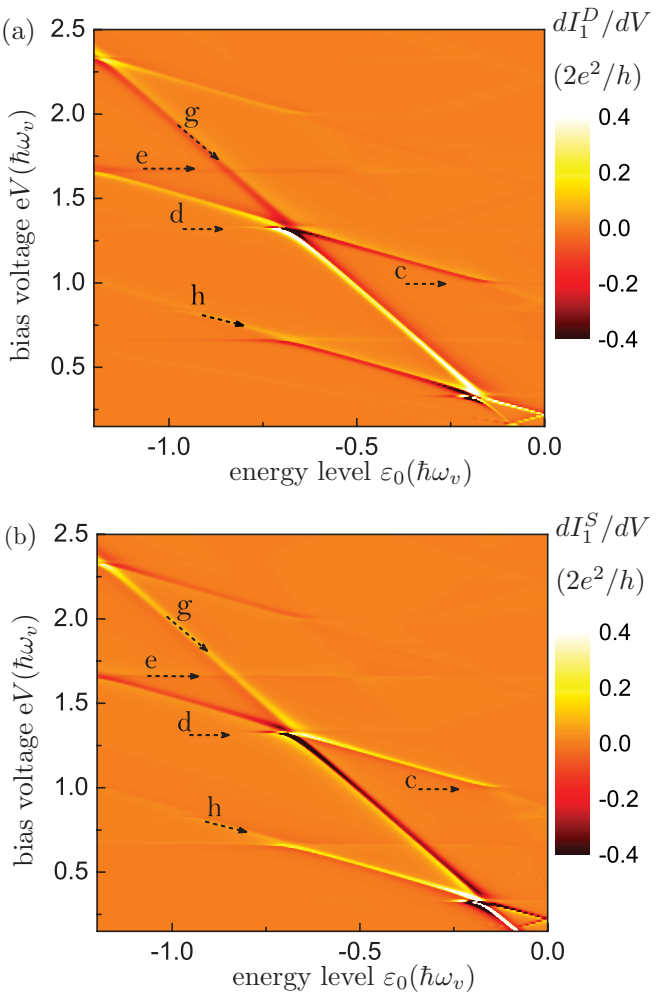

FIG. 5. (Color online) Density plot of the ac differential conductance of (a) the dissipative Josephson current I_1^D and (b) the nondissipative Josephson current I_1^S vs the molecular energy level ε_0 and the bias voltage V. The parameters are identical to those used for Fig. 2(b).

of resonant tunneling at the gap edges with singular DOS.[1] Feature f instead shows a broader structure without negative differential conductance since the occupation of the final state is different, namely nearly empty for f and nearly full for g. Moreover, we identify another pronounced feature "h" moving with ε_0, as well as one of its replicas. The underlying picture is shown in Fig. 4(h). An electron starting from the molecular level emits a vibron and is Andreev reflected. One could say that the electron traverses the bias voltage V one and a half times. Accordingly, the feature has an unusual slope of $\partial eV/\partial\varepsilon_0 = -2/3$. Assuming that the molecular level is shifted by a gate voltage V_g as $\varepsilon_0 = \varepsilon_0' - eV_g$, we predict the distinctive slope $\partial V/\partial V_g = 2/3$ of this feature in a bias-voltage/gate-voltage map. Interestingly, the feature is confined to the voltage range $\hbar\omega_v \leqslant eV \leqslant \hbar\omega_v + 2\Delta$. This is due to the fact that for $eV > \hbar\omega_v + 2\Delta$, electrons prefer direct tunneling, while for $eV < \hbar\omega_v$, the process is blocked due to the Pauli principle.

B. Differential conductance of the ac Josephson current

We finally turn to the ac Josephson current. In Fig. 5 we plot the differential conductances of the dissipative and nondissipative components as functions of V and ε_0 for small Γ, where the decoupling approximation is valid. The features seen in Fig. 2(b) for the dc current are found again. However, their appearance is different: Feature f becomes blurred in the ac case and feature h is visible in a much broader voltage range.

More interestingly, we observe an approximate *antiperiodic* behavior of both the dissipative and the nondissipative components of the ac differential conductance as functions of the bias voltage. The ac current itself exhibits the same antiperiodicity (not shown). The antiperiod in eV is the vibron energy $\hbar\omega_v$.

This means that the alternating current and the ac differential conductance change their phase by π whenever eV is increased by $\hbar\omega_v$. This antiperiodicity is a direct consequence of the polaronic effect: The anomalous (off-diagonal) self-energies in Eqs. (16) and (17) contain a factor $(-1)^l$. This factor stems from the corresponding factor in the anomalous correlation function of the polaron-shift operators, Eq. (11). As noted above, the factor is due to Andreev reflection since an outgoing electron and an Andreev-reflected hole couple to the vibron with opposite sign. For the weak molecule-lead coupling considered here, the current is dominated by processes involving a single vibron number l determined by V. According to Eqs. (16) and (17), there is then an effective phase difference across the MJJ of $2eVt/\hbar + l\pi$. The alternating current then contains a factor of $\sin(2eVt/\hbar + l\pi)$. As a result, the sign of the ac Josephson current depends on the even-odd parity of the vibron number l. The phase of the ac components can be measured with established techniques[24] or employing the coupling to a charge qubit, as proposed recently.[25] Our results are related to the long-standing $\cos\varphi$ problem:[24,25] It was found that the measured result for the phase of the ac Josephson current does not agree with theoretical predictions. In the present work we have identified a mechanism by which this phase could even change periodically as a function of the bias voltage.

IV. SUMMARY

In summary we have studied the transport properties of MJJs for which the electronic tunneling rates are modified by polaron formation. Pronounced features due to its interplay with the superconductivity in the leads have been identified in the differential conductance of both the dc and ac Josephson currents. We have explained these features in terms of vibron-assisted Andreev reflection. The combination of sequential tunneling and Andreev reflection leads to conductance peaks that show an unusual shift of their peak bias voltage with the molecular energy level or gate voltage, $V \sim (2/3)\, V_g$. Furthermore, the opposite sign of the coupling of electrons and Andreev-reflected holes to vibrons induces periodic phase changes of the ac components of the Josephson current—their phase changes by π when the bias voltage eV is increased by one vibrational energy quantum $\hbar\omega_v$. We propose to search for this clear-cut polaronic effect by measuring the ac Josephson current through molecular junctions.

ACKNOWLEDGMENTS

B.H.W. is grateful for the support by the NSFC (Grant No. 11074266) and the Fundamental Research Funds for the Central Universities. J.C.C. is supported by the 863 Program (Project No. 2011AA010205), the NSFC (Grants No. 61131006 and No. 61021064), the Major National Development Project of Scientific Instrument and Equipment (Grant No. 2011YQ150021), the major project (Project No. YYYJ-1123-1), and the Shanghai Municipal Commission of Science and Technology (Project No. 10JC1417000). C.T. acknowledges useful discussions with P. M. R. Brydon and financial support by the Deutsche Forschungsgemeinschaft, in part through Research Unit 1154, *Towards Molecular Spintronics*.

*bhwu2010@gmail.com
†carsten.timm@tu-dresden.de

[1] S. De Franceschi, L. Kouwenhoven, C. Schönenberger, and W. Wernsdorfer, Nat. Nanotech. **5**, 703 (2010).
[2] A. Martín-Rodero and A. Levy Yeyati, Adv. Phys. **60**, 899 (2011).
[3] T. Novotný, A. Rossini, and K. Flensberg, Phys. Rev. B **72**, 224502 (2005).
[4] J. A. van Dam, Y. V. Nazarov, E. P. A. M. Bakkers, S. De Franceschi, and L. P. Kouwenhoven, Nature (London) **442**, 667 (2006).
[5] A. Zazunov, R. Egger, C. Mora, and T. Martin, Phys. Rev. B **73**, 214501 (2006).
[6] A. Marchenkov, Z. Dai, B. Donehoo, R. N. Barnett, and U. Landman, Nat. Nanotech. **2**, 481 (2007).
[7] H. I. Jørgensen, T. Novotný, K. Grove-Rasmussen, K. Flensberg, and P. E. Lindelof, Nano Lett. **7**, 2441 (2007).
[8] J. Sköldberg, T. Löfwander, V. S. Shumeiko, and M. Fogelström, Phys. Rev. Lett. **101**, 087002 (2008).
[9] V. V. Mkhitaryan and M. E. Raikh, Phys. Rev. B **77**, 195329 (2008).
[10] C. Benjamin, T. Jonckheere, A. Zazunov, and T. Martin, Eur. Phys. J. B **57**, 279 (2007).
[11] I. G. Lang and Y. A. Firsov, Sov. Phys. JETP **16**, 1301 (1963).
[12] G. D. Mahan, *Many-Particle Physics* (Plenum, New York, 1990).
[13] M. Galperin, M. A. Ratner, and A. Nitzan, J. Phys.: Condens. Matter **19**, 103201 (2007).
[14] J. Rammer, *Quantum Field Theory of Non-equilibrium States* (Cambridge University Press, Cambridge, 2007).
[15] J. C. Cuevas, A. Martín-Rodero, and A. Levy Yeyati, Phys. Rev. B **54**, 7366 (1996).
[16] Q.-F. Sun, H. Guo, and J. Wang, Phys. Rev. B **65**, 075315 (2002).
[17] B. Wang, J. Wang, and H. Guo, Phys. Rev. Lett. **82**, 398 (1999).
[18] Y. X. Xing, B. Wang, and J. Wang, Phys. Rev. B **82**, 205112 (2010).
[19] Z.-Z. Chen, R. Lü, and B.-F. Zhu, Phys. Rev. B **71**, 165324 (2005).
[20] K. Flensberg, Phys. Rev. B **68**, 205323 (2003).
[21] A. Zazunov and T. Martin, Phys. Rev. B **76**, 033417 (2007).
[22] M. Octavio, M. Tinkham, G. E. Blonder, and T. M. Klapwijk, Phys. Rev. B **27**, 6739 (1983).
[23] J. C. Cuevas and W. Belzig, Phys. Rev. Lett. **91**, 187001 (2003).
[24] A. Barone and G. Paterno, *Physics and Applications of the Josephson Effect* (Wiley, New York, 1982), and references therein.
[25] J. Leppäkangas, M. Marthaler, and G. Schön, Phys. Rev. B **84**, 060505(R) (2011).